

Article

Areal Surface Roughness of AZ31B Magnesium Alloy Processed by Dry Face Turning: An Experimental Framework Combined with Regression Analysis

Honghong Gao *, Baoji Ma *, Ravi Pratap Singh and Heng Yang

School of Mechatronic Engineering, Xi'an Technological University, Xi'an 710021, China; staticravi78@gmail.com (R.P.S.); yh752606754@163.com (H.Y.)

* Correspondence: gaohonghong@xatu.edu.cn (H.G.); mabaojee@163.com (B.M.)

Received: 2 February 2020; Accepted: 14 May 2020; Published: 16 May 2020



Abstract: Surface roughness is used to quantitatively evaluate the surface topography of the workpiece subjected to mechanical processing. The optimal machining parameters are critical to getting designed surface roughness. The effects of cutting speed, feed rate, and depth of cut on the areal surface roughness of AZ31B Mg alloys were investigated via experiments combined with regression analysis. An orthogonal design was adopted to process the dry turning experiment of the front end face of the AZ31B bar. The areal surface roughness S_a and S_z of the end face were measured with an interferometer and analyzed through direct analysis and variance analysis (ANOVA). Then, an empirical model was established to predict the value of S_a through multiple regression analysis. Finally, a verification experiment was carried out to confirm the optimal combination of parameters for the minimum S_a and S_z , as well as the availability of the regression model for predicting S_a . The results show that both S_a and S_z of the machined end face reduce with the decrease in feed rate. The minimum of S_a and S_z reaches to 0.577 and 5.480 μm , respectively, with the cutting speed of 85 m/min, the feed rate of 0.05 mm/rev, and a depth of cut of 0.3 mm. The feed rate, depth of cut, and cutting speed contribute the greatest, the second and the smallest to S_a , respectively. The linear regression model can predict S_a of AZ31B machined with dry face turning, since the cutting speed, feed rate and depth of cut can explain 97.5% of the variation of S_a .

Keywords: surface roughness; magnesium alloys; machining; ANOVA; regression analysis

1. Introduction

Magnesium (Mg) alloys have been widely used in many industrial fields, such as electronics, automobile, and aerospace, due to their low density, high specific strength, and thermal conductivity, superior damping, and electromagnetic shielding performance [1,2]. Mg alloys are also extensively studied in the biomedical fields as potential implant materials, due to their excellent biocompatibility, biodegradability, and similar mechanical properties with bone [3–5]. When Mg alloys need to be machined as potential biomaterials, it is better to keep the surface from reaction with other substances during machining, since magnesium tends to have chemical reactions and forms hydrogen in contact with water-based coolants, which is extremely flammable. Additionally, oil-based lubricants introduce the danger of oil mist explosions [6,7]. Thus, the machining conditions should be carefully designed to keep the machining process safe and avoid surface deterioration. Moreover, the conventional machining process generally produces a low quality of surface integrity characterized by high surface roughness values [8]. Therefore, further surface modification is proposed to provide better surface integrity to satisfy the demand for the implant material. However, the machined surface topography influences the surface integrity induced by subsequent surface modification [9]. The machined

surface topography affects the mechanical performance of contact interfaces in subsequent surface burnishing or rolling, as well as the biomechanical function in final use [10,11]. The dry machining surface topography of magnesium-calcium implant influences the surface integrity formed by surface burnishing [12]. Therefore, the good surface topography of Mg alloys is expected via surface machining, such as turning or milling. Surface roughness is always used to evaluate the surface topography after machining. Usually, the smaller the surface roughness, the better the surface topography. The influence of the machining parameters on the surface roughness needs to be carefully studied to optimize the machining process and get the expected surface topography.

The machining process for the expected surface topography is complex because it is influenced by many factors, such as cutting conditions, cutting tool shapes and materials, cutting parameters, etc. In some researches, lubrication or coolants were used to take away the cutting heat during the machining process [13,14]. However, the surface of Mg alloys may react with the lubrication or coolants during machining, which will deteriorate the surface integrity and influence the subsequent study [15]. Thus, Mg alloys prefer to be machined in dry conditions to avoid surface deterioration in some conventional machining, such as turning and milling.

Some researches focused on the effects of dry cutting parameters on surface roughness Ra. As one of the two-dimension (2D) parameters of surface roughness, Ra represents the arithmetic mean of the absolute values of the deviation of the surface profile from the mean line in the vertical direction [16]. A higher cutting speed combined with lower feed rate results in smaller surface roughness of MgCa3.0 subjected to the cylindrical turning process [17]. The surface roughness of AZ61 Mg alloy machined via cylindrical turning is influenced by the feed rate, followed by the cutting speed and depth of cut. The increase of the feed rate or the depth of cut leads to the increase of surface roughness, whereas the increase of the cutting speed leads to the decrease of surface roughness [18]. It is indicated that the machining parameters, such as cutting speed, feed rate, and depth of cut have synergetic effects on the surface roughness of Mg alloys [19].

Some researches were carried out to investigate the effect of main cutting parameters on surface roughness aiming to estimate optimal parameters and get designed surface roughness. To get surface roughness of UNSM11311 Mg alloy between 0.8 and 1.6 μm , the optimum cutting parameter for the feed rate is 0.15 mm/rev in dry turning [20]. For the intermittent turning of UNSM11917 Mg alloy, the feed rate was identified as the most significant factor and the cutting speed was not found significant on surface roughness (Ra and Rt) [21]. In another study based on Taguchi technology and statistical experiments, feed rate had the greatest effect on the surface finish of UNSM11311 by cylindrical turning [22]. The feed rate is the most important parameter to explain the surface roughness, while no clear influence was found for the cutting speed [23]. These researches show some significant effects of parameters on Ra in the cylindrical turning of Mg alloys.

Although Ra remains the parameter of choice in a lot of papers about surface roughness, it is not the best representative of the surface quality because of the high dependence on the position of the measurements [24]. Therefore, there has been a drive towards three-dimension (3D) topographical characterization of surfaces with new standards defining area parameters [25]. The surface topography, alongside the 3D functional parameters, influence the performance of the machined surface [26]. Surface topography is 3D in nature, which can represent the natural characteristics of a surface and describe the surface more comprehensively.

As one of the 3D characterization parameters of surface roughness, areal surface roughness Sa is most commonly used to quantitatively describe surface topography. It is the arithmetic mean of the absolute values of the surface deviations from the mean plane as described in (1), which is used to detect variations in the surface [27,28].

$$Sa = \frac{1}{A} \int_0^x \int_0^y |Z(x, y)| dx dy, \quad (1)$$

where A is the sampling area.

Sa is the average surface roughness evaluated over the complete 3D surface. It can provide visual images and the mechanism of surface formation of the surveyed surface [29]. For surface quality analysis, some other areal surface parameters were also used to further understand the feature of the surface. Sz is the peak to valley height of the areal surface as described in (2), which has an increased probability of finding the worst surface roughness. By comparing the line profile roughness parameters Ra and Rz with the areal equivalents Sa and Sz, Soady K.A., etc. found Sz is generally larger than Rz after processing tempered martensitic steel [30]. Therefore, Sz can be an indication of the worst case of a surface and a reference for setting up appropriate cutting parameters. It is indicated the greater probability of finding significant surface features using areal measurement than line measurement.

$$Sz = Sp + Sv, \quad (2)$$

where Sp and Sv is the peak and valley value of the areal surface roughness, respectively.

Therefore, it is necessary to investigate the effects of cutting parameters on the areal surface roughness of the biomedical Mg alloy in dry face turning. Mg alloys with good surface quality could be prepared with proper machining parameters if effective experiment design and some optimization strategies were developed. Thus, in this research, the effects of dry turning parameters (cutting speed, feed rate, and depth of cut) on areal surface roughness (Sa and Sz) were investigated to evaluate the topography of the machined end face of AZ31B Mg alloy. First, the cermet cutting tool was selected and the face turning program was scheduled. The orthogonal experiment was designed and performed. The surface roughness of Sa and Sz was measured with an interferometer. Then, the influences of dry turning parameters on Sa and Sz were investigated by statistical analysis. The optimal combination of dry turning parameters was obtained based on the minimal value of Sa and Sz. A linear regression model was established to predict Sa of AZ31B machined with dry face turning. Finally, a verification experiment was carried out to confirm the optimal combination of parameters and the availability of the regression model for predicting areal surface roughness Sa.

2. Materials and Methods

2.1. Workpiece Materials and Cutting Tools

Extruded AZ31B bars with a length of 100 mm and a diameter of 30 mm were used as the workpiece in this research. The front end face of the workpiece was machined with a dry turning method. The nominal chemical composition (wt.%) of the AZ31B is 2.96 Al, 0.52 Zn, 0.31 Mn, 0.16 Si, 0.006 Cu, 0.003 Fe, 0.001 Ni, and balance Mg. The presence of Al and Zn can improve the creep resistance of AZ31B. Although the biocompatibility of Al is limited, it seems to be a valid alloying element for AZ31B in body contact, since it can reduce the corrosion rate of the Mg alloys by stabilizing hydroxides in chloride environments [31]. Mg alloys with 9 wt.% of aluminum showed enhanced osteoblastic activity in the surrounding guinea pig femora. Small amounts of aluminum released continuously during the degradation process might be tolerable [32]. Therefore, the biosecurity of the presence of Al less than 3 wt.% in AZ31B is acceptable.

Smaller surface roughness reaches when the cermet tool, compared with a cemented carbide tool, was utilized to machine stainless steel, due to the higher hardness, toughness, wear-resistance, and better thermo-stability [33]. Therefore, the ultrafine cermet tool (NX2525, Mitsubishi Corporation, Tokyo, Japan) was selected in this research for the continuous dry turning of AZ31B. The NX2525 is a triangular ultrafine cermet insert with a negative rake, 0° relief angle, and nose radius of 0.4 mm. Its hardness is up to 92.2 HRA and bending strength is up to 2.0 GPa [34]. Thus, it can be used in both low-speed and high-speed dry turning.

2.2. Machining Process and Experiment Design

The dry turning was performed on a three-axis lathe (CKD6136i, Dalian Machine Tool Group Co., LTD, Dalian, China) equipped with numerical control (NC) system. The workpiece is clamped by the

three-jaw chuck. The maximum allowable rotational speed of the spindle is 3000 rpm. The cutting tool fixed on the rest can move along X and Z directions. In the face turning, the workpiece rotates with the spindle at a speed of no more than 3000 rpm. The cutting tool first moves the depth of cut from the end face to $-Z$ direction and then feeds along $-X$ direction until it reaches the center of the front end face of the workpiece. The schematic diagram of the face turning is shown in Figure 1.

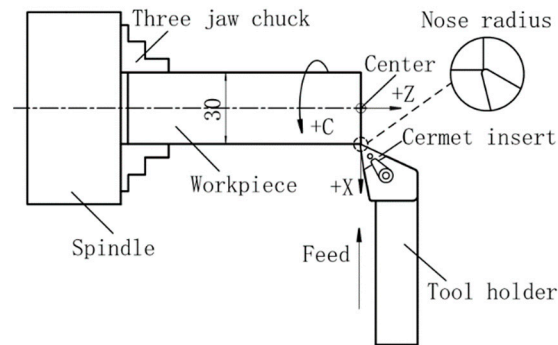


Figure 1. Schematic diagram of face turning.

In this experiment, cutting speed (factor A), feed rate (factor B), and depth of cut (factor C) were selected as the influence factors. Three levels were set for each factor, as shown in Table 1. In this face turning experiment, the cutting speed for each workpiece was kept constant at the set level by programming with NC code 'G96'. The rotational speed rises with the feed movement and it was kept within 3000 rpm by using NC code 'G50'. For example, 'G96 S85' was programmed to keep the linear cutting speed constant at 85 m/min. 'G50 S3000' was placed in front of 'G96 S85' to limit the rotational speed within 3000 rpm when the distance between the cutting point and the center of the front end face is smaller than 4.5 mm. Otherwise, the cutting speed will exceed 3000 rpm. Thus, there is a speed limit area on each end face, in which the cutting speed is smaller than the set level.

Table 1. Factors and levels of the dry turning parameters.

Level	Factor		
	A Cutting Speed (m/min)	B Feed Rate (mm/rev)	C Depth of Cut (mm)
1	$A_1 = 47$	$B_1 = 0.05$	$C_1 = 0.2$
2	$A_2 = 66$	$B_2 = 0.08$	$C_2 = 0.3$
3	$A_3 = 85$	$B_3 = 0.11$	$C_3 = 0.4$

An orthogonal design method was utilized to organize the dry turning experiment. Thus, nine combinations of the parameters in the dry turning experiment are presented in Table 2.

2.3. Areal Surface Roughness Measurement

The areal surface roughness parameters (S_a and S_z) are adopted to describe the surface topography of the AZ31B after dry face turning in this work. A white-light interferometer (Zegage Plus, Zygo, Middlefield, CT, USA) was used to measure the 3D surface roughness of the frontal surfaces of the samples after face turning. Zegage Plus is a 3D optical profiler with non-contact 3D coherence scanning interferometry (CSI). The optical resolution (transverse) is $0.95 \mu\text{m}$ with a 10X standard objective. The sampling area is $0.834 \times 0.834 \text{ mm}$ without additional filtering. Figure 2 presents the front end faces of samples 1 to 9.

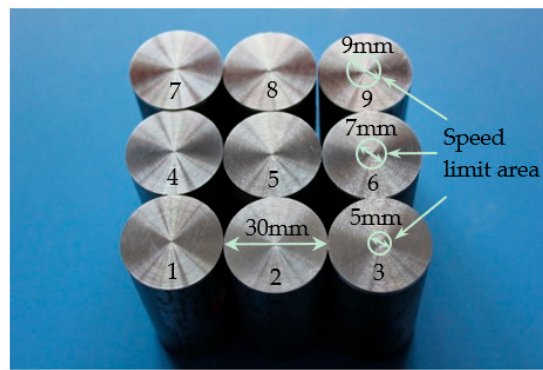


Figure 2. Image of the front end faces of samples 1 to 9.

The white circles on samples 3, 6, and 9 indicate the speed limit areas corresponding to the cutting speed at 47, 66, and 85 m/min, respectively. Therefore, three sampling areas are selected outside the speed limit area of the front end face of each sample, to make sure the cutting speed is consistent with the set value. The images of 3D surface topography and the values of S_a and S_z were obtained with the interferometer. By calculating the measured values of S_a and S_z from three sampling areas, the average of each sample was obtained, followed by the standard deviation (SD). The results are presented in Table 2.

Table 2. The orthogonal experiment design and measurement results.

Sample	Factor			Measured Values of S_a (S_z) ¹ , μm			Averages and SD of S_a (S_z), μm
	A	B	C	Area 1	Area 2	Area 3	
1	1	1	1	0.655 (8.130)	0.698 (8.165)	0.614 (9.791)	0.656 ± 0.042 (8.695 ± 0.949)
2	1	2	2	0.996 (12.691)	0.911 (8.934)	0.884 (11.084)	0.930 ± 0.058 (10.903 ± 1.885)
3	1	3	3	1.521 (16.929)	1.481 (12.951)	1.472 (15.196)	1.491 ± 0.026 (15.025 ± 1.994)
4	2	1	2	0.599 (7.401)	0.521 (6.647)	0.663 (8.973)	0.594 ± 0.071 (7.674 ± 1.187)
5	2	2	3	1.012 (11.338)	0.969 (10.937)	1.109 (11.694)	1.030 ± 0.072 (11.323 ± 0.379)
6	2	3	1	1.590 (12.852)	1.427 (10.934)	1.431 (11.635)	1.483 ± 0.093 (11.807 ± 0.970)
7	3	1	3	0.762 (7.553)	0.571 (7.955)	0.538 (5.260)	0.624 ± 0.121 (6.923 ± 1.454)
8	3	2	1	1.038 (9.638)	0.958 (8.863)	0.970 (10.370)	0.989 ± 0.043 (9.624 ± 0.754)
9	3	3	2	1.467 (12.510)	1.382 (9.562)	1.430 (10.928)	1.426 ± 0.043 (11.000 ± 1.475)

¹ Data in the brackets are the corresponding value for S_z (the same in the following tables).

The averages of S_a , as well as S_z , of samples 1 to 9 are different from each other, which attributes to the different combinations of the machining parameters. The smaller standard deviation means better consistency of the surface roughness of the three sampling areas. Thus, the consistency of S_a is better than that of S_z for each sample, due to the smaller standard deviation.

2.4. Multiple Linear Regression

Multiple linear regression is used to determine the linear relationship between one dependent variable and two or more independent variables. In this work, this method is utilized to find out the correlation coefficients between the areal surface roughness and the three machining factors, cutting speed, feed rate, and depth of cut, to establish a quantitative prediction model. The coefficient of the regression model is used as the goodness of fit to describe the degree of the predicted value fitting to the measured value. The closer the coefficient is to 1, the better the model fits.

3. Results and Discussion

3.1. Direct Analysis and Range Analysis

The smaller S_a and S_z indicate better surface topography. According to the averages of S_a and S_z of samples 1 to 9 in Table 2, the average of S_z nearly 10 times that of S_a indicates S_z can reflect some

worst cases of the machined surface topography. The worst cases on the machined surfaces may be induced by the scratches of the breaking chips. Sample 3 (the combination of $A_1B_3C_3$) has the worst surface topography, due to the maximal S_a and S_z (1.491 and 15.025 μm , respectively). Sample 4 (the combination of $A_2B_1C_2$) has the minimal S_a (0.594 μm), while Sample 7 (the combination of $A_3B_1C_3$) has the minimal S_z (6.923 μm). In this case, it cannot determine which one (Sample 4 or Sample 7) has a better surface topography, according to the averages of S_a and S_z . From a statistical point of view, the orthogonal experiment results need to be further analyzed to find a better combination of the parameters that maybe results in smaller S_a and S_z . Therefore, a direct analysis was used to seek for the optimal combination of the three factors. The results are presented in Table 3.

Table 3. The results of direct analysis and range analysis for S_a and S_z .

Item	Factor		
	A	B	C
\bar{K}_1	1.026 (11.541)	0.625 (7.764)	1.042 (10.042)
\bar{K}_2	1.036 (10.268)	0.983 (10.617)	0.984 (9.859)
\bar{K}_3	1.013 (9.182)	1.467 (12.611)	1.048 (11.090)
Range	0.023 (2.359)	0.842 (4.847)	0.065 (1.230)

where \bar{K}_i ($i = 1, 2, 3$) is defined as the arithmetic mean of S_a (or S_z) for each factor at each level i . The minimum \bar{K}_i means the smallest surface roughness when a factor takes level i . Range value for a factor is the difference between the maximum and the minimum among $\bar{K}_1, \bar{K}_2, \bar{K}_3$. Take S_a for example, \bar{K}_1 for factor B (0.625 μm) is the arithmetic mean of 0.656, 0.594 and 0.624 μm ($\bar{K}_{1B} = (0.656 + 0.594 + 0.624)/3 = 0.625$). The range for factor B (0.842 μm) is the difference between the maximum (\bar{K}_{3B}) and the minimum (\bar{K}_{1B}). $\bar{K}_{3A}, \bar{K}_{1B}, \bar{K}_{2C}$ is the minimum among the \bar{K}_i ($i = 1, 2, 3$) for factors A, B, and C, respectively.

The influence of each level on the arithmetic means (i.e., \bar{K}_i) of S_a and S_z for each factor are depicted in Figure 3. The small variation of \bar{K}_i for S_a shows with the increase of cutting speed and depth of cut from level 1 to 3 in Figure 3a. \bar{K}_i of S_z decreases with the increase in cutting speed from level 1 to 3, as shown in Figure 3b. The increase of depth of cut leads to a slight decrease in \bar{K}_i for S_a and S_z from level 1 to 2, and then an increase from level 2 to 3. The SD of the \bar{K}_i of S_a , as well as that of S_z for the feed rate is smallest compared with that for the other two factors. It indicates the averages of S_a , as well as that of S_z , are well consistent with each other at the same feed rate.

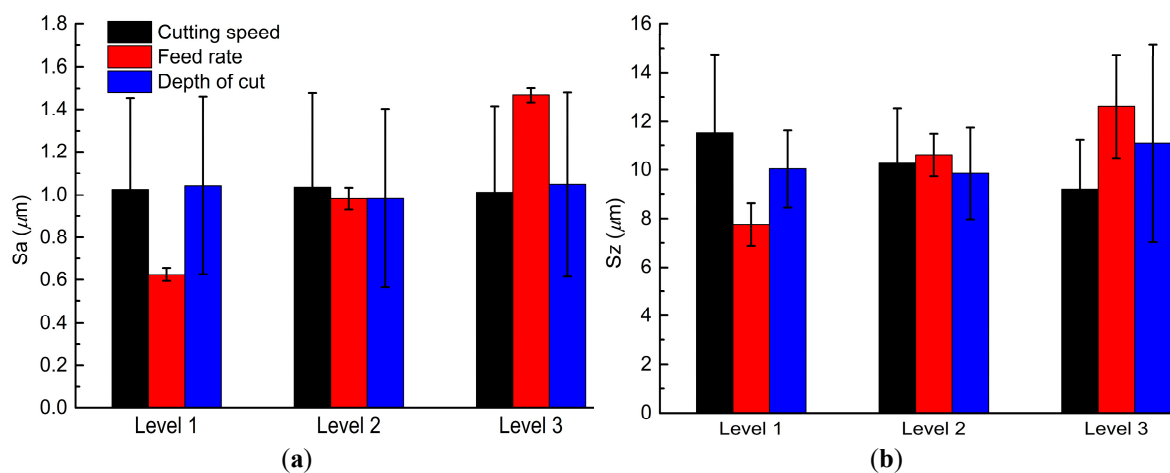


Figure 3. The influence of each level on the arithmetic mean of S_a (a) and S_z (b) for each factor.

It is worth noting that the \bar{K}_i of S_a and S_z consistently increases with the increased feed rate from level 1 to level 3. Both the \bar{K}_i of S_a and that of S_z reach to the smallest, when the cutting speed, feed

rate, and depth of cut takes level 3 ($\overline{K3_A}$), level 1 ($\overline{K1_B}$), and level 2 ($\overline{K2_C}$), respectively. Therefore, the combination of $A_3B_1C_2$ will probably result in smaller values of both Sa and Sz than that of $A_2B_1C_2$ and $A_3B_1C_3$.

Range analysis is used to determine the importance of the three factors to the areal surface roughness Sa and Sz. In Table 3, the range of factor B is the largest (0.842 for Sa and 4.847 μm for Sz). It indicates that the feed rate has the greatest effect on both Sa and Sz among all the three factors. The range of factor A is the smallest (0.023 μm) for Sa, indicating cutting speed has the least effect on Sa. The range of factor C is the smallest (1.230 μm) for Sz, which means the depth of cut has the least effect on Sz.

3.2. ANOVA Analysis

Although range analysis can explain the importance of each factor on Sa and Sz, there is no objective criterion to evaluate the range. Thus, it is uncertain that the variation of the experiment results should be attributed to the variation of the factors or the random error. In this case, ANOVA analysis is used to investigate the significance of the three factors to the areal surface roughness Sa and Sz with the significance level of 0.05 ($F_{0.05}(2, 2) = 19$). If the F-value of a factor is larger than $F_{0.05}(2, 2)$, or the P-value is smaller than 0.05, the factor has a significant effect on the result. The ANOVA analysis results of Sa and Sz are shown in Table 4.

Table 4. ANOVA analysis results of Sa and Sz.

Factor	Square Sum of Dispersion	df ¹	Mean Square Error	F-Value ²	P-Value ³
A	0.0008 (8.3657)	2	0.0004 (4.1828)	0.8276 (8844.6160)	0.5472 (0.0001)
B	1.0719 (35.6070)	2	0.5359 (17.8035)	1133.2236 (37645.3894)	0.0009 (0.0000)
C	0.0077 (2.6490)	2	0.0038 (1.3245)	8.0980 (2800.6372)	0.1099 (0.0004)
Experiment Error	0.0009 (1.2064)	2	0.0005 (0.6032)	-	-

¹ The abbreviation of the degree of freedom. ² The result of the homogeneity test for the variance. ³ The probability of samples obtained when the hypothesis is true.

The P-value of factor B is 0.0009 for Sa, which is much smaller than 0.05. It confirms that feed rate has a significant effect on the averages of Sa via dry turning process. The P-value of factor A for Sa is 0.5472 and that of factor C is 0.1099, which indicates that both cutting speed and depth of cut have a negligible effect on the averages of Sa. The P-values of factors A, B, and C are all much smaller than 0.05 for Sz, which indicates the three factors have significant effects on the Sz of AZ31B via dry turning process.

3.3. Regression Model of Sa

All the standard deviations and experimental errors of Sa are smaller than that of Sz in the above direct and ANOVA analysis. Thus, Sa is more appropriate for evaluating the whole surface topography and establishing a prediction model for surface roughness of AZ31B via dry face turning. The coefficients for evaluating the goodness of fit of the multiple regression model of Sa are listed in Table 5.

Table 5. Coefficients for evaluating the goodness of fit of the regression model of Sa.

R	R ²	Adjusted R ²	Standard Error
0.992	0.984	0.975	0.058

In Table 5, the coefficient R reaches to 0.992 with the standard error 0.058, indicating the model fits the data well. It can be used to predict the areal surface roughness of AZ31B by face turning in

dry conditions. The adjusted R^2 is 0.975, which means the variation of the factors (i.e., cutting speed, feed rate, and depth of cut) can at least account for 97.5% variation of S_a . Then, ANOVA analysis was performed to test the validity of the regression model.

The significance test is performed with the significance level of 0.05 and the F-value ($F_{0.05}(3, 5) = 5.41$). Table 6 shows the ANOVA analysis results of the regression model. The F-value of this model is 103.953, which is much larger than $F_{0.05}(3, 5)$. It confirms that the regression model of S_a is valid. It also can be confirmed valid according to its significance (far less than 0.05).

Table 6. ANOVA analysis results of the multiple regression model.

Model	Sum of Squares	df	Mean Square	F-Value	Significance
Regression analysis	1.064	3	0.355	103.953	0.000
Residual	0.017	5	0.003	-	-
Total	1.081	8	-	-	-

The coefficients of this multiple linear regression model are shown in Table 7. Therefore, the empirical model of S_a is described as (3).

$$Y = -0.084 - 0.00035X_A + 14.033X_B + 0.028X_C, \quad (3)$$

where dependent variable Y represents the areal surface roughness S_a (μm), independent variables X_A , X_B , and X_C represent the cutting speed (m/min), the feed rate (mm/rev), and the depth of cut (mm), respectively. The intercept (B_0) is $-0.084 \mu\text{m}$. The non-standardized coefficient B_i ($i = 1, 2, 3$) means the predicted value of Y increases by $B_i \mu\text{m}$ for every one unit increase of X_A ($i = 1$), X_B ($i = 2$), or X_C ($i = 3$). Therefore, the unit of the right side is the same as that of the left side in Equation (3).

Table 7. Coefficients of the multiple linear regression model of S_a .

Item	Non-standardized Coefficient		Standardized Coefficient	t	P-Value
	B	Standard Error			
Intercept	-0.084	0.128	-	-0.659	0.539
Cutting speed	-0.00035	0.001	-0.015	-0.266	0.801
Feed rate	14.033	0.795	0.992	17.657	0.000
Depth of cut	0.028	0.238	0.007	0.119	0.910

The non-standardized coefficient cannot directly reflect the significance of each independent variable to the dependent variable, due to different units and ranges of the three independent variables. According to the standardized coefficients in Table 7, the feed rate can account for 99.2% of S_a . Cutting speed combining with the depth of cut only explains about 0.8% of S_a . The correlation of S_a with feed rate, depth of cut, cutting speed is the greatest, the second, the smallest, respectively.

The P -value of feed rate is less than 0.05, which also indicates the feed rate is the most significant factor affecting S_a among the three factors. They are consistent with the previous conclusions drawn from range and ANOVA analysis.

3.4. Verification Experiment

According to the direct analysis, $A_3B_1C_2$ is supposed to be the best combination of the parameters for the smallest values of S_a and S_z . To verify the analysis result, another sample (No. 10) was machined with the combination of $A_3B_1C_2$, i.e., the cutting speed of 85 m/min, the feed rate of 0.05 mm/rev, and the depth of cut of 0.3 mm. The areal surface topographies from three sampling areas of sample 10 are shown in Figure 4a–c. The visual images give us a direct understanding of the surveyed surface, including tooth marks, feed directions, distance between peak and valley. It is observed that the surface

topography in Figure 4c is more consistent than that in Figure 4a,b, which is confirmed by the smallest S_a and S_z compared with the corresponding values from another two images.

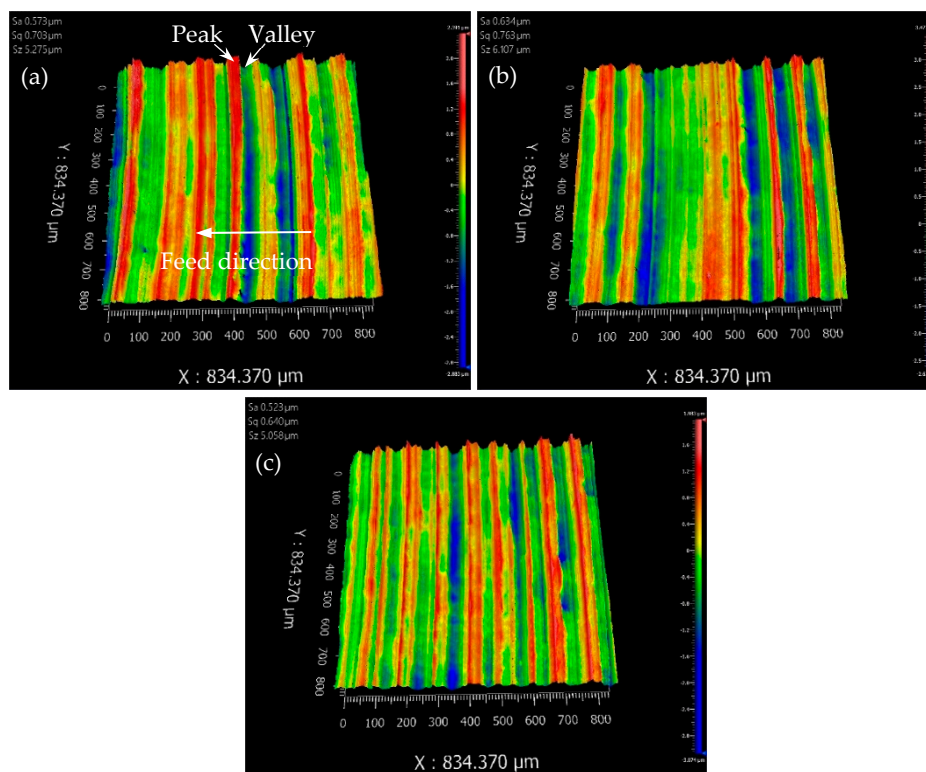


Figure 4. The images of the areal surface roughness of the verified sample 10: (a), (b), and (c) is from the first, the second and the third sampling area, respectively.

The measured values of S_a from the three sampling areas are 0.573, 0.634, and 0.523 μm , respectively. The average of S_a is 0.577 ± 0.056 μm (with SD), which is 1.7% smaller than that (0.594 μm) resulted from $A_2B_1C_2$. The measured values of S_z from the three sampling areas are 5.275, 6.107, and 5.058 μm , respectively. The average of S_z is 5.480 ± 0.554 μm , which is 28.6% smaller than that (6.923 μm) resulted from $A_3B_1C_3$. Therefore, the combination of $A_3B_1C_2$ is verified to be the optimal combination for obtaining minimal S_a and S_z . In the case of the feed rate at the lowest level, higher cutting speed (from level 2 to level 3) results in a slight decrease of S_a and a large decrease of S_z . Lower depth of cut (from level 3 to level 2) results in a relatively large decrease of S_a and a small decrease of S_z . These effects of the two nonsignificant factors on S_a and S_z are consistent with the relationship got from range, ANOVA, and regression analysis.

Moreover, Equation (3) was used to predict the S_a of sample 10 with the parameter values of $A_3B_1C_2$, to verify the availability of the empirical prediction model. The calculated S_a is 0.596 μm , with the 3% relative error from the measured value (0.577 μm). Therefore, the empirical model of S_a can accurately predict the areal surface roughness S_a of AZ31B after dry face turning with the given machining parameters.

4. Conclusions

The effects of different dry turning parameters (cutting speed, feed rate, and depth of cut) on the areal surface roughness S_a and S_z of AZ31B magnesium alloy was investigated in this paper. The following conclusions were drawn from the experimental analysis and linear regression model:

1. The optimal machining parameters of AZ31B was obtained through the direct analysis of the orthogonal experiment results since a smaller surface roughness means better surface topography. Both S_a and S_z reduce with the decrease in feed rate. The smallest S_a of 0.577 μm and S_z of 5.480 μm

were obtained in the verification experiment with the cutting speed at level 3 (85 m/min), feed rate at level 1 (0.05 mm/rev), and depth of cut at level 2 (0.3 mm). The results verify that $A_3B_1C_2$ is the optimal combination of the machining parameters.

2. Range and ANOVA analysis results show that the feed rate, depth of cut, and cutting speed contribute the greatest, second, and smallest to the value of S_a , respectively. The feed rate, cutting speed, and depth of cut contribute the greatest, second, and smallest to the value of S_z , respectively. Feed rate is the most significant parameter for both S_a and S_z .

3. An empirical model of S_a is established by multiple linear regression analysis. S_a can be accurately predicted with this model since the variation of the three factors can at least account for 97.5% variation of S_a . The availability of this model is confirmed by the verification experiment.

This research provides an approach to explore the optimal combination of dry turning parameters for the smallest areal surface roughness of AZ31B Mg alloy. It also maps the relationship between areal surface roughness and processing parameters. Thus, an experimental framework combined with regression analysis was established to predict the areal surface roughness and get the expected surface topography for biomedical AZ31B subjected to dry face turning.

Author Contributions: Conceptualization, H.G. and B.M.; methodology, H.G.; validation, H.G., R.P.S., and H.Y.; data analysis, H.G.; writing—original draft preparation, H.G.; writing—review and editing, H.G., B.M., R.P.S., and H.Y.; visualization, H.G.; funding acquisition, H.G. and B.M. All authors have read and agreed to the published version of the manuscript.

Funding: This research was funded by the Key Laboratory Program of Education Department of Shaanxi Province (19JS035) and the Key Research and Development Program of Shaanxi Province (2018GY-120).

Acknowledgments: Thanks go to Tao Qiang, School of Materials Science and Chemical Engineering, Xi'an Technological University, for polishing the English language.

Conflicts of Interest: The authors declare no conflict of interest.

References

1. Gray, J.E.; Luan, B. Protective coatings on magnesium and its alloys—a critical review. *J. Alloys Compd.* **2002**, *336*, 88–113. [[CrossRef](#)]
2. Wu, C.S.; Zhang, Z.; Gao, F.H.; Zhang, L.J.; Zhang, J.Q.; Cao, C.N. Study on the anodizing of AZ31 magnesium alloys in alkaline borate solutions. *Appl. Surf. Sci.* **2007**, *253*, 3893–3898. [[CrossRef](#)]
3. Han, H.S.; Loffredo, S.; Jun, I.; Edwards, J.; Kim, Y.C.; Seok, H.K.; Witte, F.; Mantovani, D.; Glyn-Jones, S. Current status and outlook on the clinical translation of biodegradable metals. *Mater. Today* **2019**, *23*, 57–71. [[CrossRef](#)]
4. Alvarez-lopez, M.; Pereda, M.D.; del Valle, J.A.; Fernandez-Lorenzo, M.; Garcia-Alonso, M.C.; Ruano, O.A.; Escudero, M.L. Corrosion behaviour of AZ31 magnesium alloy with different grain sizes in simulated biological fluids. *Acta Biomater.* **2010**, *6*, 1763–1771. [[CrossRef](#)]
5. Hou, X.N.; Qin, H.F.; Gao, H.Y.; Mankoci, S.; Zhang, R.X.; Zhou, X.F.; Ren, Z.C.; Doll, G.L.; Martini, A.; Sahai, N.; et al. A systematic study of mechanical properties, corrosion behavior and biocompatibility of AZ31B Mg alloy after ultrasonic nanocrystal surface modification. *Mater. Sci. Eng. C* **2017**, *78*, 1061–1071. [[CrossRef](#)]
6. Tönshoff, H.K.; Friemuth, T.; Winkler, J.; Podolsky, C. Improving the characteristics of magnesium work pieces by burnishing operations. *Magnes. Alloys Appl.* **2006**, 406–411. [[CrossRef](#)]
7. Pedersen, W.; Ramulu, M. Facing SiCp/Mg metal matrix composites with carbide tools. *J. Mater. Process. Technol.* **2006**, *172*, 417–423. [[CrossRef](#)]
8. Yao, C.; Ma, L.; Du, Y.; Ren, J.; Zhang, D. Surface integrity and fatigue behavior in shot-peening for high speed milled 7055 aluminum alloy. *Proc. IMechE Part B J. Eng. Manuf.* **2015**, *1*, 1–14. [[CrossRef](#)]
9. Schulze, V.; Bleicher, F.; Groche, P.; Guo, Y.B.; Pyun, Y.S. Surface modification by machine hammer peening and burnishing. *CIRP Ann. Manuf. Technol.* **2016**, *65*, 809–832. [[CrossRef](#)]
10. Li, P.G.; Zhai, Y.F.; Huang, S.K.; Wang, Q.D.; Fu, W.P.; Yang, H.P. Investigation of the contact performance of machined surface morphology. *Tribol. Int.* **2017**, *107*, 125–134. [[CrossRef](#)]

11. Niemczewska-Wójcik, M.; Piekoszewski, W. The surface texture and its influence on the tribological characteristics of a friction pair: Metal-polymer. *Arch. Civ. Mech. Eng.* **2017**, *17*, 344–353. [[CrossRef](#)]
12. Salahshoor, M.; Guo, Y.B. Surface integrity of magnesium-calcium implants processed by synergistic dry cutting-finish burnishing. *Procedia Eng.* **2011**, *19*, 288–293. [[CrossRef](#)]
13. Suneesh, E.; Sivapragash, M. Parameter optimisation to combine low energy consumption with high surface integrity in turning Mg/Al₂O₃ hybrid composites under dry and MQL conditions. *J. Braz. Soc. Mech. Sci.* **2019**, *41*, 89. [[CrossRef](#)]
14. Akhyar, G.; Purnomo, B.; Hamni, A.; Harun, S.; Burhanuddin, Y. The machined surface of magnesium AZ31 after rotary turning at air cooling condition. In Proceedings of the 3rd International Conference on Science, Technology, and Interdisciplinary Research (IC-STAR), University of Lampung, Indonesia, 18–20 September 2017.
15. Uddin, M.S.; Rosman, H.; Hall, C.; Murphy, P. Enhancing the corrosion resistance of biodegradable Mg-based alloy by machining-induced surface integrity: Influence of machining parameters on surface roughness and hardness. *Int. J. Adv. Manuf. Technol.* **2016**, *90*, 2095–2108. [[CrossRef](#)]
16. Soady, K.A.; Mellor, B.G.; Shackleton, J.; Morris, A.; Reed, P.A.S. The effect of shot peening on notched low cycle fatigue. *Mater. Sci. Eng. A* **2011**, *528*, 8579–8588. [[CrossRef](#)]
17. Denkena, B.; Lucas, A. Biocompatible magnesium alloys as absorbable implant materials-adjusted surface and subsurface properties by machining processes. *CIRP Ann. Manuf. Technol.* **2007**, *56*, 113–116. [[CrossRef](#)]
18. Mustea, G.; Brabie, G. Influence of cutting parameters on the surface quality of round parts made from AZ61 magnesium alloy and machined by turning. *Adv. Mater. Res.* **2014**, *837*, 128–134. [[CrossRef](#)]
19. Wojtowicz, N.; Danis, I.; Monies, F.; Lamesle, P.; Chieragati, R. The influence of cutting conditions on surface integrity of a wrought magnesium alloy. *Procedia Eng.* **2013**, *63*, 20–28. [[CrossRef](#)]
20. Villeta, M.; Agustina, B.; Pipaón, J.M.S.; Rubio, E.M. Efficient optimisation of machining processes based on technical specifications for surface roughness application to magnesium pieces in the aerospace industry. *Int. J. Adv. Manuf. Technol.* **2012**, *60*, 1237–1246. [[CrossRef](#)]
21. Carou, D.; Rubio, E.M.; Lauro, C.H.; Davim, J.P. Experimental investigation on surface finish during intermittent turning of UNSM11917 magnesium alloy under dry and near dry machining conditions. *Measurement* **2014**, *56*, 136–154. [[CrossRef](#)]
22. Villeta, M.; Rubio, E.M.; Sáenz De Pipaón, J.M.; Sebastián, M.A. Surface finish optimization of magnesium pieces obtained by dry turning based on Taguchi techniques and statistical tests. *Mater. Manuf. Process.* **2011**, *26*, 1503–1510. [[CrossRef](#)]
23. Carou, D.; Rubio, E.M.; Lauro, C.H.; Davim, J.P. Experimental investigation on finish intermittent turning of UNSM11917 magnesium alloy under dry machining. *Int. J. Adv. Manuf. Technol.* **2014**, *75*, 1417–1429. [[CrossRef](#)]
24. Librera, E.; Riva, G.; Safarzadeh, H.; Previtali, B. On the use of areal roughness parameters to assess surface quality in laser cutting of stainless steel with CO₂ and fiber sources. *Procedia CIRP* **2015**, *33*, 532–537. [[CrossRef](#)]
25. Child, D.J.; West, G.D.; Thomson, R.C. Assessment of surface hardening effects from shot peening on a Ni-based alloy using electron backscatter diffraction techniques. *Acta Mater.* **2011**, *59*, 4825–4834. [[CrossRef](#)]
26. Nieslony, P.; Krolczyk, G.M.; Wojciechowski, S.; Chudy, R.; Zak, K.; Maruda, R.W. Surface quality and topographic inspection of variable compliance part after precise turning. *Appl. Surf. Sci.* **2018**, *434*, 91–101. [[CrossRef](#)]
27. Gong, M.; Rao, S.Z.; Li, L. Effects of machining parameters on surface roughness of joints in manufacturing structural finger-jointed lumber (in Chinese). *J. Forest. Eng.* **2017**, *2*, 10–18.
28. Moon, J.; Yi, G.; Oh, C.; Lee, M.; Lee, Y.; Kim, M. A new technique for three-dimensional measurements of skin surface contours evaluation of skin surface contours according to the aging process using a stereo image optical topometer. *Phys. Meas.* **2002**, *23*, 247–259. [[CrossRef](#)]
29. He, B.F.; Ding, S.Y.; Wei, C.E.; Liu, B.X.; Shi, Z.Y. Review of measurement methods for areal surface roughness. *Opt. Precis. Eng.* **2019**, *27*, 78–93. (In Chinese)
30. Soady, K.A.; Mellor, B.G.; West, G.D.; Harrison, G.; Morris, A.; Reed, P.A.S. Evaluating surface deformation and near surface strain hardening resulting from shot peening a tempered martensitic steel and application to low cycle fatigue. *Int. J. Fatigue* **2013**, *54*, 106–117. [[CrossRef](#)]
31. Makar, G.L.; Kruger, J. Corrosion of magnesium. *Int. Mater. Rev.* **2017**, *38*, 138–153. [[CrossRef](#)]

32. Witte, F.; Kaese, V.; Haferkamp, H.; Switzer, E.; Meyer-Lindenberg, A.; Wirth, C.J.; Windhagen, H. In vivo corrosion of four magnesium alloys and the associated bone response. *Biomaterials* **2005**, *26*, 3557–3563. [[CrossRef](#)] [[PubMed](#)]
33. Noordin, M.Y.; Venkatesh, V.C.; Sharif, S. Dry turning of tempered martensitic stainless tool steel using coated cermet and coated carbide tools. *J. Mater. Process. Technol.* **2007**, *185*, 83–90. [[CrossRef](#)]
34. Hsu, C.Y.; Lin, Y.Y.; Lee, W.S.; Lo, S.P. Machining characteristics of Inconel 718 using ultrasonic and high temperature-aided cutting. *J. Mater. Process. Technol.* **2008**, *198*, 359–365. [[CrossRef](#)]



© 2020 by the authors. Licensee MDPI, Basel, Switzerland. This article is an open access article distributed under the terms and conditions of the Creative Commons Attribution (CC BY) license (<http://creativecommons.org/licenses/by/4.0/>).